

Metamaterial Inspired CPW Fed Compact Low-Pass Filter

Basil J. Paul^{1, *}, Shanta Mridula¹, Binu Paul¹, and Pezhohil Mohanan²

Abstract—A metamaterial inspired co-planar waveguide (CPW) fed compact low-pass filter is presented in this paper. The 3 dB cutoff frequency of the filter is 1.4 GHz. The roll-off rate achieved for this filter is 47.4 dB/GHz. Sharp roll-off is obtained by introducing an additional resonance using an inductor in series with the shunt capacitor. The usage of chip inductor also results in a compact filter structure. The overall filter dimensions are 39 mm × 32 mm × 1.6 mm. The filter uses defected ground structure (DGS) for attaining stop band attenuation. The measured insertion loss of the filter in the pass band is less than 0.8 dB and average stop band attenuation is better than 23 dB. The equivalent circuit of the proposed filter is similar to that of a dual-CRLH (D-CRLH) transmission line.

1. INTRODUCTION

Low-pass filter is an inevitable component of any communication system. The need for compact low-pass filters is never ending as the size of communication devices is getting smaller and smaller. With the increasing demand for small hand held devices, miniaturization of microwave components has become an interesting topic among RF Engineers. Commonly used microstrip filters available in literature are stepped impedance filters [1], filters with defected ground structure (DGS) [2, 3] etc. In [4] a microstrip low-pass filter using Hilbert shaped complementary single split ring has been proposed. In [5–7] CRLH transmission lines using various forms of CSRR have been reported. This paper presents a compact low-pass filter designed using metamaterial. The equivalent circuit of the filter is similar to that of a dual composite right left handed (D-CRLH) transmission line. The proposed low-pass filter incorporates chip inductor for improving the roll-off rate and DGS for improving the stop band attenuation.

2. THEORY

A simple low-pass filter consists of a combination of inductance L and capacitance C and the filter output is tapped across the capacitor as shown in Figure 1(a). The S_{21} response of the filter is shown in Figure 1(d). The drawback of such a simple low-pass filter is the poor roll-off rate. The roll-off of such a low-pass filter can be improved by introducing an additional resonance using an inductor in series with the shunt capacitor as shown in Figure 1(b). The improvement in the roll-off is clear from the S_{21} response of the filter shown in Figure 1(e). The handicap of this circuit is the poor stop band attenuation. The stop band attenuation can be improved by introducing a parallel combination of inductor and capacitor in the series arm as shown in Figure 1(c). The improved low-pass response with better roll-off and improved stop band attenuation is shown in Figure 1(f).

The filter circuit in Figure 1(c) is similar to the equivalent circuit of a D-CRLH transmission line. The equivalent circuit of a CRLH transmission line and its dual counterpart [8, 9] is shown in Figures 2(a), (b).

Received 20 March 2015, Accepted 29 May 2015, Scheduled 5 June 2015

* Corresponding author: Basil J. Paul (basiljpaul@gmail.com).

¹ Division of Electronics Engineering, School of Engineering, Cochin University of Science and Technology, India. ² Department of Electronics, Cochin University of Science and Technology, India.

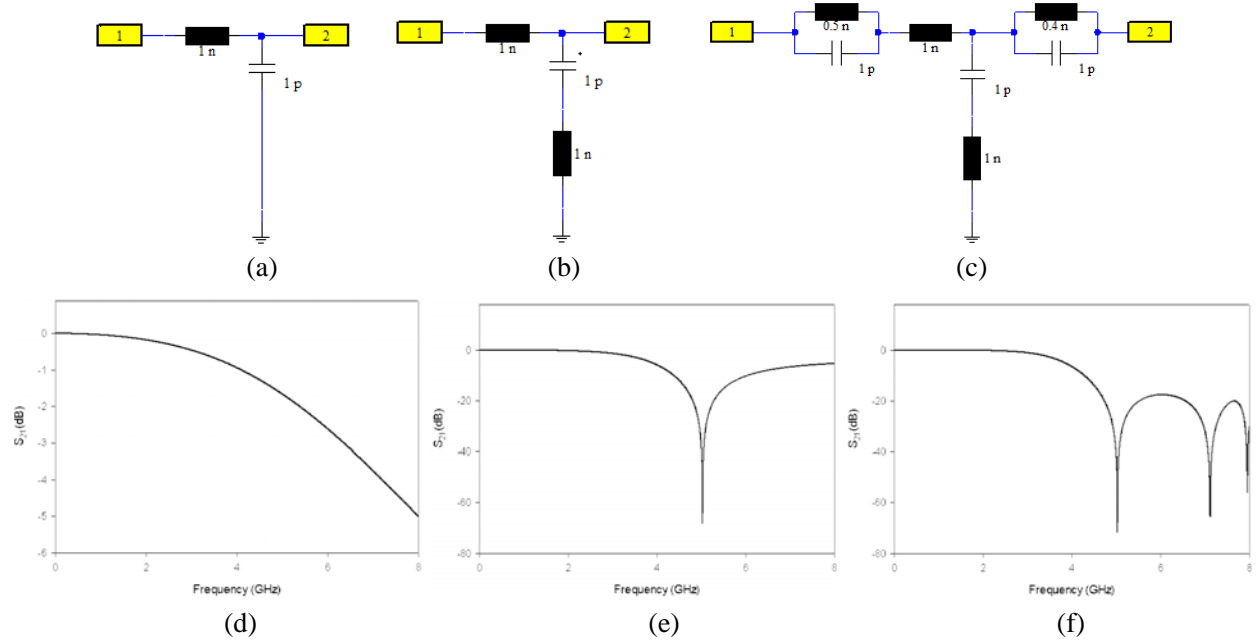


Figure 1. (a) Circuit model of a conventional LC low-pass filter; (b) circuit model of conventional LC low-pass filter with inductor for introducing notch; (c) circuit model of conventional low-pass filter with notch and transmission zeros in stop band; (d) transmission characteristics of circuit model-(a); (e) transmission characteristics of circuit model-(b); (f) transmission characteristics of circuit model-(c).

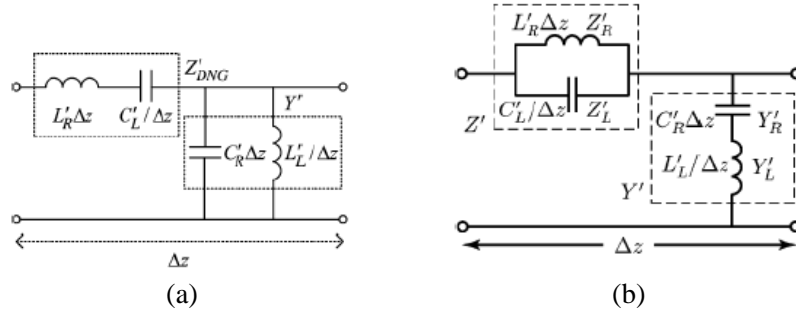


Figure 2. Equivalent circuit. (a) CRLH transmission line; (b) dual of CRLH transmission line.

3. GEOMETRY OF THE LOW-PASS FILTER

The proposed low-pass filter geometry is shown in Figure 3(a). The structure is designed on a substrate with $\epsilon_r = 4.4$, $\tan \delta = 0.02$ and thickness 1.6 mm. The dimensions of the various elements are $L = 39$ mm, $W = 32$ mm, $w_c = 5.5$ mm, $l_c = 14$ mm, $l_t = 5.5$ mm, $w_t = 3$ mm, $g_1 = 0.5$ mm, $g_2 = 15$ mm, $g_3 = 0.3$ mm, $w_g = 3$ mm, $w_1 = 3$ mm, $w_2 = 26$ mm, $w_3 = 3$ mm. It consists of a conductor backed co-planar waveguide fed transmission line with resonant elements connected in shunt. The L and C components of the low-pass filter are obtained from the equivalent inductance and capacitance of the conductor backed co-planar transmission line. The notch characteristics is obtained by introducing an additional series resonance caused by a combination of chip inductor and distributed patch capacitor in shunt with the transmission line. The chip inductor used is a 4.7 nH coil wound fixed value chip inductor by Coilcraft Inc. The simulated transmission characteristics is shown in Figure 3(b). It is clear from the graph that the structure exhibits a low-pass nature, and also a sharp notch is present in the characteristics, which is contributed by the combined effect of shunt inductance and capacitance.

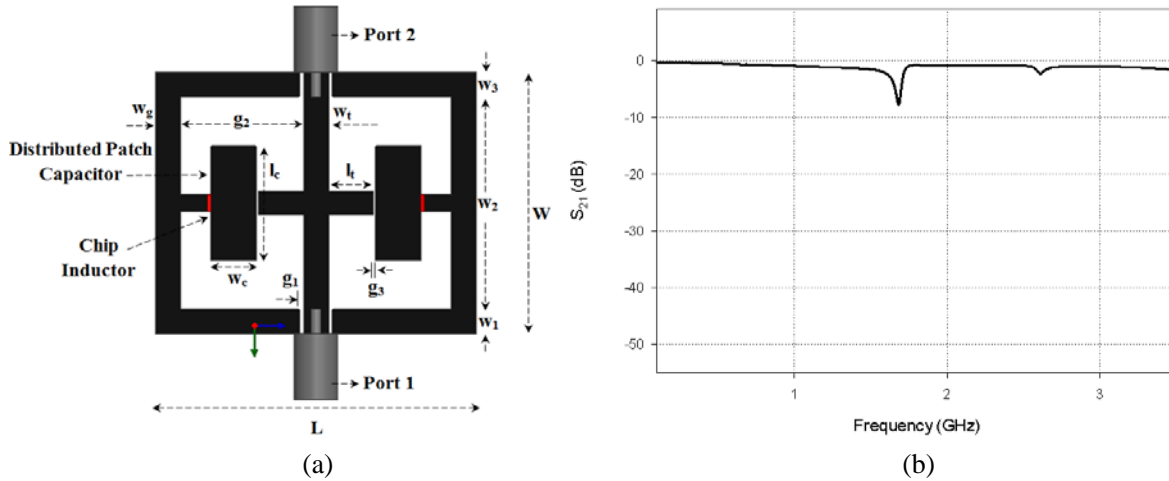


Figure 3. (a) Geometry of the low-pass filter; (b) simulated transmission characteristics.

4. GEOMETRY OF LOW-PASS FILTER WITH DGS

From the transmission characteristics in Figure 3(b) it is clear that the stop band attenuation is poor. As mentioned in Section 2, parallel LC circuits can be used to improve the stop band attenuation. Defected Ground Structures (DGS) in the bottom ground plane are equivalent to parallel LC circuits in the series arm. In the proposed filter, dumb bell shaped DGS structures are used in the bottom plane in order to improve the stop band attenuation. The DGS on conductor backing is shown in Figure 4(b). The dimensions of DGS are $w_{d1} = 4\text{ mm}$, $w_{l1} = 4\text{ mm}$, $w_{d2} = 6.5\text{ mm}$, $w_{l2} = 6.5\text{ mm}$, $t_{d1} = 0.3\text{ mm}$, $t_{d2} = 0.3\text{ mm}$, $l_{d1} = 11\text{ mm}$, $l_{d2} = 13.5\text{ mm}$. The top plane of the filter shown in Figure 4(a) is same as that explained in Section 3.

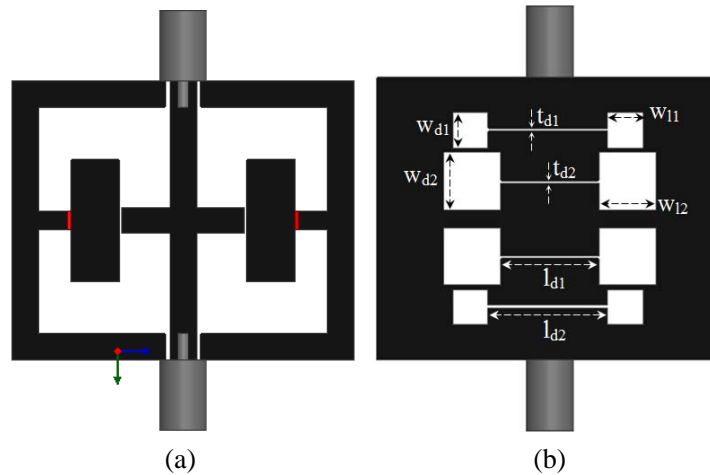


Figure 4. Complete structure of the proposed low-pass filter. (a) Top plane; (b) bottom plane.

The narrow line connecting two square shaped sections acts as capacitor and the square shaped region acts as the inductor. Since the thin line acts as capacitor, electric field is concentrated in this area. The magnetic field is concentrated around the square shaped inductor section. The field distributions are shown in Figure 5. The transmission characteristics of the proposed low-pass filter is shown in Figure 6. It is clear from the transmission curve that the stop band attenuation has improved when compared with the one that does not have DGS.

The surface field distributions on the top plane at a pass-band frequency 406.6 MHz and at the

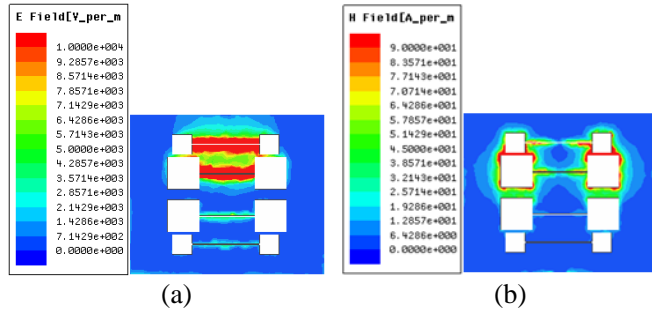


Figure 5. Electric and Magnetic field distribution on DGS embedded ground. (a) Electric field; (b) magnetic field.

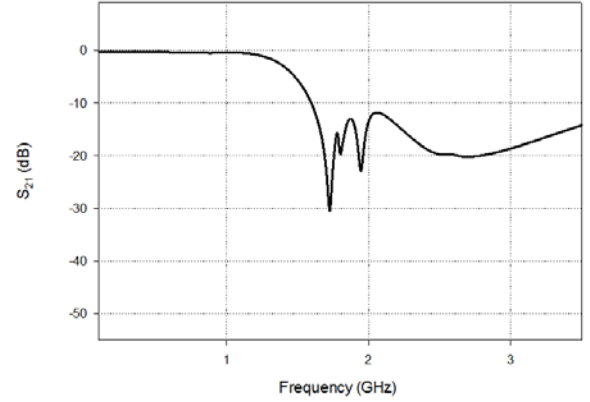


Figure 6. Simulated transmission characteristics of the proposed low pass filter.

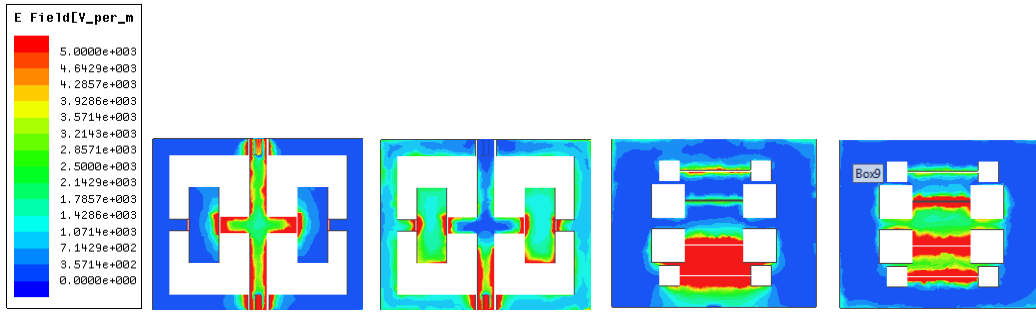


Figure 7. Surface field distribution of top plane at 406.6 MHz & 1.72 GHz and bottom plane at 1.79 GHz & 2.06 GHz.

first transmission zero frequency 1.72 GHz and bottom plane at stop band frequencies 1.79 GHz and 2.06 GHz are shown in Figure 7. It is clear from the field plot that there exists a good coupling between port 1 and port 2 at pass-band frequency 406.6 MHz. At 1.72 GHz, LC circuit connected in shunt is at resonance and the coupling between port 1 and port 2 is poor. At the stop band frequencies DGS elements are excited resulting in poor coupling between port 1 and port 2 as shown in Figure 7.

5. LUMPED CIRCUIT MODEL OF THE FILTER

The lumped circuit model of the filter is shown in Figure 8. The mutual coupling between individual elements in the structure is not taken into consideration.

The transmission line of width 3 mm in the top plane as shown in Figure 3(a) is equivalent to series inductance and shunt capacitance. The entire transmission line is split into three conductor backed CPW transmission line sections, indicated as w_1 , w_2 , w_3 in Figure 3(a). The inductance and capacitance introduced by these section are indicated as L_{w1} , L_{w2} , L_{w3} , C_{w1} , C_{w2} and C_{w3} in Figure 8. In the first and last section the separation between transmission line and the CPW ground is 0.5 mm, indicated as g_1 . The length of these section is 3 mm. In the middle section w_2 , separation between transmission line and CPW ground is 15 mm indicated as g_2 . The length of this section is 26 mm. The characteristic impedance and effective permittivity of a conductor backed CPW transmission line is given by Equations (1)–(6) [10].

$$\text{Characteristic impedance, } Z_0 = \frac{60\pi}{\sqrt{\epsilon_{eff}}} \frac{1}{\frac{K(k)}{K(k')} + \frac{K(k_1)}{K(k'_1)}} \quad (1)$$

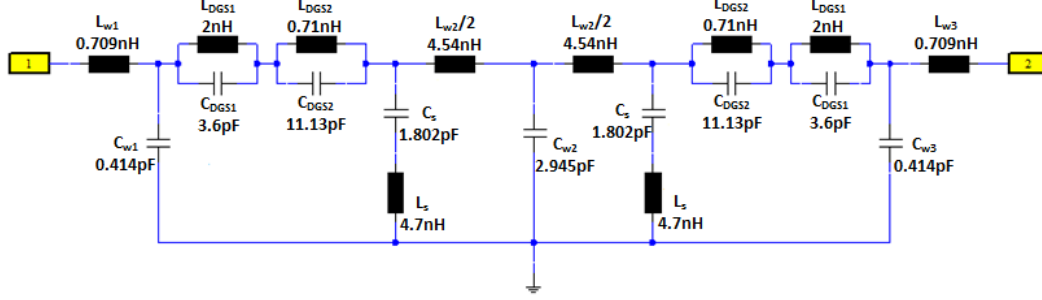


Figure 8. Equivalent circuit model of the filter.

$$\text{Effective permittivity, } \epsilon_{eff} = \frac{1 + \epsilon_r \frac{K(k')}{K(k)} \frac{K(k_1)}{K(k'_1)}}{1 + \frac{K(k')}{K(k)} \frac{K(k_1)}{K(k'_1)}} \quad (2)$$

where $K(k)$ and $K(k')$ are elliptic integrals of first kind and its complement.

$$K'(k) = K(k') \quad (3)$$

$$k = \frac{w_t}{g_1 + w_t + g_1} \quad \text{for sections } w_1 \text{ and } w_3$$

$$k = \frac{w_t}{g_2 + w_t + g_2} \quad \text{for section } w_2 \quad (4)$$

where w_t is the transmission line width and g_1 and g_2 is the gap between transmission line and the CPW ground.

$$k_1 = \frac{\tanh\left(\frac{\pi w_t}{4h}\right)}{\tanh\left(\frac{\pi(g_1 + w_t + g_1)}{4h}\right)} \quad \text{for sections } w_1 \text{ and } w_3$$

$$k_1 = \frac{\tanh\left(\frac{\pi w_t}{4h}\right)}{\tanh\left(\frac{\pi(g_2 + w_t + g_2)}{4h}\right)} \quad \text{for section } w_2 \quad (5)$$

$$k' = \sqrt{1 - k^2}, \quad k'_1 = \sqrt{1 - k_1^2} \quad (6)$$

The characteristic impedance and phase velocity of a loss less transmission line is related to per unit length line parameters L_{pul} (Henry/meter) and C_{pul} (Farads/meter) as

$$\text{Characteristic impedance, } Z_0 = \sqrt{\frac{L_{pul}}{C_{pul}}} \quad (7)$$

$$\text{Phase velocity, } V_p = \frac{1}{\sqrt{L_{pul}C_{pul}}} = \frac{c}{\sqrt{\epsilon_{eff}}} \quad (8)$$

L_{pul} and C_{pul} can be calculated using Equations (1), (2), (7) and (8). L and C for each section of transmission line is found by multiplying it with corresponding transmission line length. The sharp roll-off in the stop band is introduced by shunt capacitance and inductance connected in series. It is indicated as L_s and C_s in Figure 8. The inductance used is 4.7 nH chip inductor. The first transmission zero is obtained at 1.72 GHz. The capacitance introduced by the distributed patch capacitor is calculated from

$$f = \frac{1}{2\pi\sqrt{L_s C_s}} \quad (9)$$

DGS structures used for improving stop band attenuation is modeled as parallel LC circuit labeled as L_{DGS} and C_{DGS} in Figure 8. The design equations used for computing L_{DGS} and C_{DGS} are [11]

$$C_{DGS} = \frac{\omega_c}{2Z_0(\omega_0^2 - \omega_c^2)} \quad (10)$$

$$L_{DGS} = \frac{1}{\omega_0^2 C_{DGS}} \quad (11)$$

where ω_0 is the resonant frequency of the parallel LC circuit and ω_c is the 3 dB cutoff frequency.

6. EXPERIMENTAL RESULTS AND DISCUSSION

The proposed filter is fabricated and tested in the laboratory. The fabricated filter is shown in Figure 9(a). The measured S_{11} and S_{21} of the filter are shown in Figure 9(b). The simulated and circuit model characteristics are also included for comparison. The filter geometry is designed and simulated using Ansys HFSS and circuit model is designed and simulated using CST Design Studio. The first transmission zero at 1.8 GHz is the combined effect of series chip inductor and distributed

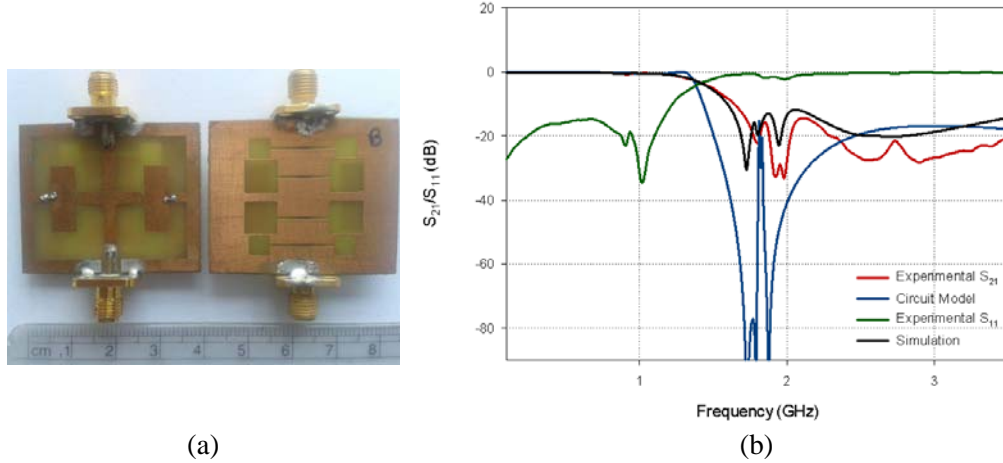


Figure 9. (a) Top and bottom plane of the fabricated filter; (b) S_{11} and S_{21} response of the filter.

Table 1. Performance comparison of the proposed filter with other filters already reported.

Parameter	Proposed filter	[1]	[2]	[4]	[12]	[13]
Cutoff frequency (GHz)	1.4	2	3.2	2.15	2.4	3.75
Size of DGS (mm ²)	24 × 6.5 21.5 × 4	Not used	4.5 × 11.5 2.7 × 7.9 2.3 × 6.9	7 × 8 to 3.5 × 4 (9 H-CSSRR cells)	14.7 × 3.8 13 × 4	20 × 15
Roll-off (dB/GHz)	47.4	18.8	34	68	30.9	30.9
Insertion loss	< 0.8 dB 0.01–1.2 GHz	< 0.7 dB dc–1.7 GHz	Not specified	< 0.59 dB	< 0.3 dB Not specified	< 2 dB dc–3.5 GHz
Stop band attenuation	> 23 dB (avg) 1.78–3.5 GHz	> 20 dB 2.9–4.65 GHz	> 20 dB 3.7–8 GHz	> 20 dB 2.45–25 GHz	> 20 dB 2.95–8.25 GHz	> 20 dB 4.3–15.8 GHz
ϵ_r, t (mm)	4.4, 1.6	10.2, -	10, 1.575	2.2, 0.78	3.38, 0.813	4.4, 1.6

capacitance. The transmission zeros beyond 1.8 GHz are caused by the DGS structures. The measured 3 dB cut-off frequency of the filter is 1.4 GHz. The roll-off rate measured is 47.4 dB/ GHz. The insertion loss of the filter is better than 0.8 dB in the pass band up to 1.2 GHz. The return loss of the filter is better than 14.6 dB in the pass band. The average stop band attenuation of the filter is better than 23 dB.

The roll-off rate of the proposed filter is better than the reported works [1, 2, 12, 13] as shown in Table 1. The pass-band insertion loss is comparable with [1, 4] and is much better than [13]. The overall size of the proposed filter is 39 mm × 32 mm, which is compact for low cutoff frequency and is designed using commonly available low-permittivity substrate. In the stop band the major drawback is the occurrence of two overshoots at 1.85 GHz and 2.1 GHz.

7. CONCLUSION

A compact low-pass filter is presented in this paper. Low insertion loss in pass band and good stop band attenuation are the highlights of the proposed filter. The usage of chip inductor provides a sharp roll-off within a compact structure. The major drawback of the proposed filter is the ripples at the starting of stop band frequencies. The further improvement of stop band attenuation and reduction of stop band ripple is currently under investigation.

ACKNOWLEDGMENT

The authors would like to thank Kerala State Council for Science Technology and Environment (KSCSTE) for providing financial assistance for this research work as per Council File No. 03/FSHP/2013/CSTE, dated 10/01/2014.

REFERENCES

1. Hsieh, L. H. and K. Chang, "Compact low pass filter using stepped impedance hair pin resonator," *Electronics Letters*, Vol. 37, No. 14, 899–900, 2001.
2. Liu, H. W., Z. F. Li, X. W. Sun, and J. F. Mao, "An improved 1-D periodic defected ground structure for microstrip line," *IEEE Microwave and Wireless Components Letters*, Vol. 14, No. 4, 180–182, 2004.
3. Kufa, M. and Z. Raida, "Low pass filter with reduced fractal defected ground structure," *Electronics Letters*, Vol. 49, No. 3, 899–900, 2013.
4. Xu, H. X., G. M. Wang, C. X. Zhang, and Q. Peng, "Hilbert shaped complementary single split ring resonator and low-pass filter with ultra wide stopband, excellent selectivity and low insertion-loss," *International Journal of Electronics and Communications*, Vol. 65, No. 11, 901–905, 2011.
5. Xu, H. X., G. M. Wang, Z. M. Xu, X. Chen, Z. Yu, and L. Geng, "Dual shunt branch circuit and harmonic suppressed device application," *Applied Physics A*, Vol. 108, No. 2, 497–502, 2012.
6. Xu, H. X., G. M. Wang, C. X. Zhang, and X. Wang, "Characterization of composite right/left handed transmission line," *Electronics Letters*, Vol. 47, No. 18, 1030–1032, 2011.
7. Xu, H. X., G. M. Wang, C. X. Zhang and Q. Peng, "Complementary metamaterial transmission line for monoband and dual-band bandpass filters application," *International Journal of RF and Microwave Computer-Aided Engineering*, Vol. 22, No. 2, 200–210, 2012.
8. Caloz, C., "Dual composite right/left handed (D-CRLH) transmission line metamaterial," *IEEE Microwave and Wireless Components Letters*, Vol. 16, No. 11, 585–587, 2006.
9. Park, J. H., Y. H. Ryu, J. G. Lee, and J. H. Lee, "Epsilon negative zeroth order resonator antenna," *IEEE Transactions on Antennas and Propagation*, Vol. 55, No. 12, 3710–3712, 2007.
10. Wadell, B. C., *Transmission Line Design Handbook*, Artech House Inc., Norwood, 1991.
11. Ahn, D., J. S. Park, C. S. Kim, J. Kim, Y. Qian, and T. Itoh, "A design of the low pass filter using the novel microstrip defected ground structure," *IEEE Transactions on Microwave Theory and Techniques*, Vol. 49, No. 1, 86–93, 2001.

12. Yang, J. and W. Wu, "Compact elliptic function low pass filter using defected ground structure," *IEEE Microwave and Wireless Components Letters*, Vol. 18, No. 9, 578–580, 2008.
13. Chen, H. J., T. H. Huang, C. S. Chang, L. S. Chen, N. F. Wang, Y. H. Wang, and M. P. Houn, "A novel cross shape DGS applied to design ultra wide stopband low pass filters," *IEEE Microwave and Wireless Components Letters*, Vol. 16, No. 5, 252–254, 2006.